Targeting PARP1 in XRCC1 deficient sporadic invasive breast cancer or pre-invasive ductal carcinoma in situ induces synthetic lethality and chemoprevetion

Reem Ali[1], Abdulbaqi Al-kawaz[2], Michael S Toss[2] , Andrew R Green[2], Islam M Miligy[2], Katia A Mesquita[1], Claire Seedhouse[3], Sameer Mirza[4], Vimla Band[4], Emad A Rakha[2]*, and Srinivasan Madhusudan[1,5]*

[1] Translational Oncology, Division of Cancer and Stem Cells, School of Medicine, University of Nottingham, Nottingham University Hospitals, Nottingham NG5 1PB, UK.

[2] Department of Pathology, Division of Cancer and Stem Cells, School of Medicine, University of Nottingham, Nottingham NG51PB, UK.

[3] Academic Haematology, Division of Cancer and Stem Cells, School of Medicine, University of Nottingham, Nottingham University Hospitals, Nottingham NG5 1PB, UK.

[4] Department of Genetics, Cell Biology and Anatomy, University of Nebraska Medical Centre, 985805 Nebraska Medical Centre, Omaha, NE 68198, USA.

[5] Department of Oncology, Nottingham University Hospitals, City Hospital Campus, Nottingham NG5 1PB, UK.

Running title: PARP1 targeting in XRCC1 deficient breast cancers or DCIS

Conflict of interest: The authors disclose no potential conflicts of interest

Word count: 3183

Figure: 4

Keywords: Breast cancer; DNA repair; triple negative breast cancer; XRCC1; PARP;

Olaparib: synthetic lethality; chemoprevention.

1

* Corresponding authors:

Professor Srinivasan Madhusudan

Translational Oncology, Division of Cancer and Stem Cells, School of Medicine, University

of Nottingham, Nottingham University Hospitals, Nottingham NG51PB, UK. Telephone:

+44(0)115 823 1850, Fax: +44(0)115 823 1849,

E-Mail: srinivasan.madhusudan@nottingham.ac.uk

&

Professor Emad A Rakha

Department of Pathology, Division of Cancer and Stem Cells, School of Medicine,

University of Nottingham, Nottingham University Hospitals, Nottingham NG51PB, UK,

Telephone: +44(0)115 823 1850, Fax: +44(0)115 823 1849,

E-Mail: emad.rakha@nottingham.ac.uk

2

ABSTRACT

Targeting PARP1 for synthetic lethality is a new strategy for breast cancers harboring germline mutations in BRCA. However, these mutations are rare, and reactivation of BRCA-mediated pathways may result in eventual resistance to PARP1 inhibitor therapy. Alternative synthetic lethality approaches targeting more common sporadic breast cancers and pre-invasive ductal carcinoma in situ (DCIS) are desirable. Here we show that downregulation of XRCC1, which interacts with PARP1 and coordinates base excision repair, is an early event in human breast cancer pathogenesis. XRCC1-deficient DCIS were aggressive and associated with increased risk of local recurrence. Human invasive breast cancers deficient in XRCC1 and expressing high PARP1 levels also manifested aggressive features and poor outcome. The PARP1 inhibitor Olaparib was synthetically lethal in XRCC1-deficient DCIS and invasive breast cancer cells. We conclude that targeting PARP1 is an attractive strategy for synthetic lethality and chemoprevention in XRCC1-deficient breast cancers, including pre-invasive DCIS.

3

SIGNIFICANCE

Findings show that loss of XRCC1, which is associated with more malignant DCIS, can be exploited by PARP inhibition, suggesting its application as a promising therapeutic and chemoprevention strategy in XRCC1-deficient tumor cells.

4

INTRODUCTION

Targeting poly-ADP-ribose polymerase (PARP) for synthetic lethality (SL) is an exciting new strategy in BRCA germ-line mutated breast cancers (1). However, *BRCA* germ-line mutated cancers are rare. In addition, reactivation of BRCA mediated pathways may result in eventual resistance to PARP inhibitor therapy (1). Therefore alternative synthetic lethality targets enabling the extension of this approach including in sporadic DNA repair-deficient triple-negative breast cancers (TNBCs) and pre-invasive ductal carcinoma in situ (DCIS) (2) is highly desirable.

XRCC1 (X-ray repair cross-complementing gene 1) is a critical factor in DNA base excision repair (BER) and single strand break repair (SSBR) (3, 4). XRCC1 interacts with PARP1 and coordinates BER/SSBR (5, 6). In addition, XRCC1 is also involved in alternative non-homologous end joining (alt-NHEJ) pathway for double-strand breaks (DSBs) (7) and nucleotide excision repair (8). XRCC1 deficiency delays SSB rejoining thereby leading onto SSBs, which if unrepaired, eventually to double-strand breaks (DSBs) (3, 4). In addition, XRCC1 deficiency/mutation is associated with hyper-activation of PARP1 and ataxia but no cancer predisposition was reported in these individuals (9, 10). Whether PARP1 targeting will have translational application in XRCC1 deficient breast cancers is currently unknown.

In the current study, we show that XRCC1 deficient human invasive breast cancers with high PARP1 levels have aggressive pathology and worse survival. Pre-clinically, Olaparib is synthetically lethal in XRCC1 deficient cells compared to XRCC1 proficient cell lines and 3D-spheroids. In patients with pre-invasive ductal carcinoma in situ (DCIS), XRCC1 deficiency is also linked to aggressive phenotype and recurrence. XRCC1 depletion promotes

5

invasion, epithelial-mesenchymal-transitions and increased sensitivity to Olaparib monotherapy in MCF10DCIS cells. We conclude that PARP1 targeting in XRCC1 deficient invasive cancers or DCIS is an attractive synthetic lethality and chemoprevention strategy.

6

MATERIALS AND METHODS

Compounds, reagents, clonogenic assays, cell proliferation assays, confocal microscopy, functional assays (FACS, cell cycle progression, apoptosis assays), invasion assay, migration assay and 3D-spheroid assays are described in detail in supplementary materials and methods.

Cell lines and culture: MDA-MB-231, MDA-MB-157 cells were purchased from American Type Culture Collection (ATCC, Manassas, USA). Cell lines authentication was performed by AuthentiFiler™ PCR Amplification Kit. MDA-MB-231 was cultured in minimum essential amino acids medium supplemented with 10% FBS, 1% penicillin-streptomycin, 1% L-glutamine and 1% non-essential amino acids. MDA-MB-157 was grown in IMDM medium supplemented with 15%FBS and 1% penicillin/ streptomycin). Previously well-characterized Chinese hamster (CH) ovary cells; CHO9 (wild-type), EM-C11 (XRCC1-mutant), EM-C12 (XRCC1-mutant) were a gift from Late Prof. M.Z. Zdzienicka. Cells were grown in Ham F-10 media (supplemented with 10% FBS and 1% penicillin/streptomycin). MCF10DCIS cells were cultured in Dulbecco's Modified Eagle's Medium -F12 supplemented with 10% horse serum,5mg/ml insulin, 1mg/ml cholera toxin, and 100 ug/ml epidermal growth factor EGFR, 5mg/ml hydrocortisone and 1% penicillin-streptomycin. XRCC1-deficient HeLa SilenciX cells and controls XRCC1-proficient HeLa SilenciX cells were purchased from Tebu-Bio (www.tebu-bio.com). SilenciX cells were grown in Dulbecco's Modified Eagle's Medium supplemented with 10% FBS, 1% penicillin/streptomycin, and 125 µg/mL hygromycin B. All cell lines were tested for mycoplasma routinely every 3 months using mycoProbe mycoplasma detection kit (R&D systems). All cell lines were used between 15 passages window.

7

Generation of XRCC1 knockouts using CRISPR/Cas-9 system: MDA-MB-231 and MCF-10DCIS were transfected with oligonucleotides carrying gRNA silencing XRCC1cloned in a Plv-U6g-EPCG plasmid (Sigma, UK).Briefly; cells were seeded at 50- 60 % confluency in 6 well plates overnight. Cells were transfected with 2-3 µg of DNA using Lipofectamine 3000(Invitrogen, UK) in an Opti-MEM medium. Puromycin was used as a selection marker for 14 days. MDA-MB-231 cells were selected in 10ug/ml and MCF-DCIS cells were selected in 5ug/ml puromycin.

qRT-PCR analysis of epithelial-mesenchymal transition (EMT) gene expression: Real-time PCR was performed using RT^2 Profiler EMT PCR Array for 86 EMT genes. The data was analysed as per manufacturer's recommendations (https://www.qiagen.com/us/shop/genes-and-pathways/data-analysis-center-overview-page/). RPLP0 was used for normalization of the data. All experiments were performed in duplicate.

XRCC1 expression in human invasive breast cancers and pre-invasive ductal carcinoma in situ: The study was performed in a consecutive series of 1650 patients with primary invasive breast carcinomas who were diagnosed between 1986 and 1999 and entered into the Nottingham Tenovus Primary Breast Carcinoma series. All patients were treated in a single institution and have been investigated in a wide range of biomarker studies (11-15). Supplementary Table S1 summarizes patient demographics. Supplementary treatment data 1 summarizes various adjuvant treatments received by patients in this cohort. We also evaluated an independent series of 281 ER-α negative invasive BCs diagnosed and managed at the Nottingham University Hospitals between 1999 and 2007. All patients were primarily treated with surgery, followed by radiotherapy and anthracycline chemotherapy. The characteristics of this cohort are summarised in supplementary Table S2. Tumours were

8

arrayed in tissue microarrays (TMAs) and immunohistochemically profiled for XRCC1 (15), PARP1 (14) and other biological antibodies (Supplementary-Table S3) as previously described (11-13).

A total of 776 patients with non-invasive pure DCIS (ductal carcinoma in situ) diagnosed between 1987 and 2012 were identified from the National Health System (NHS) database of the Nottingham University Hospitals. A cohort of 239 DCIS that co-exist with invasive breast cancer (IBC) as well as 50 normal breast tissues was also identified. Patients' demographics are summarised in supplementary materials.

IHC scoring and statistical analyses for patient cohorts are described in detail in supplementary methods.

Written informed consent from patients was obtained where applicable. The study was conducted in accordance with the Declaration of Helsinki and ethical approval was obtained from the Nottingham Research Ethics Committee (C202313).

9

RESULTS

XRCC1-PARP1 co-expression and aggressive human breast cancers: We have previously shown that loss of XRCC1 expression (16% of tumours) was significantly associated with high grade, absence of hormonal receptors (ER-/PgR-/AR-), presence of basal-like phenotypes, triple negative phenotypes and poor survival including in patients with triple-negative breast cancers (TNBCs) (15). We have also demonstrated that PARP1 expression is linked to aggressive breast cancers (14). XRCC1 is known to interact with PARP1 during BER (7). In addition, XRCC1 deficiency/mutation can also hyper-activate PARP1 (9). We, therefore, proceeded to investigate XRCC1-PARP1 co-expression in a large clinical breast cancer cohort.

A total of 1011 breast tumours were suitable for XRCC1-PARP1 co-expression analyses (**Figure 1A**). 451/1011 (44.6%) were XRCC1+/PARP1+, 61/1011 (6%) were XRCC1-/PARP1+, 396/1011(39.1%) were XRCC1+/PARP1- and 103/1011 (10.1 %) were XRCC1-/PARP1-. As shown in **Supplementary Table S4,** tumours that are XRCC1-/PARP+ are likely to be high grade, high mitotic index, high pleomorphism, ER-/PR- and high-risk Nottingham Prognostic Index (NPI >3.4) (all adjusted p values <0.0001). In the whole cohort (n=997), XRCC1-/PARP+ tumours had the worst breast cancer-specific survival (p<0.0001) (**Supplementary Figure S1A**). In ER+ breast cancers, XRCC1-/PARP+ tumours had the worst survival outcome (p<0.0001) (**Supplementary Figure S1B**) including in patients who had no endocrine therapy (p=0.015) (**Supplementary Figure S1C**) or endocrine therapy (p<0.0001) (**Supplementary Figure S1D**). In TNBCs (n=356), similarly, XRCC1-/PARP+ tumours had the worst survival outcome in the whole cohort (p=0.001, **Figure 1B**)

10

including in patients who had no chemotherapy (p=0.003) (**Figure 1C**) or chemotherapy (p=0.038) (**Figure 1D**).

Taken together, the data provides evidence that high PARP1 levels in XRCC1 deficient tumours is not only associated with aggressive breast cancer but also suggests that targeting PARP1 could be a promising personalized treatment strategy. To explore this possibility further we conducted detailed pre-clinical studies.

Selective toxicity of Olaparib in XRCC1 deficient cells: We evaluated a panel of XRCC1 proficient and deficient Chinese hamster [CHO9 (Wild-type), EM-C12 (XRCC1 deficient)] **(Figure 1E)**, HeLa [control and XRCC1_KD silence X cells] **(Figure 1E)** and triple negative breast cancer cells [MDA-MB-231 (XRCC1 proficient) and MDA-MB-157 (XRCC1 deficient)] **(Figure 1E).** We also generated XRCC1 knock-out (KO) MDA-MB-231 cells using a CRISPR/Cas-9 system **(Figure 1E)**. Olaparib sensitivity was investigated in clonogenic survival assays. XRCC1 deficient cells are highly sensitive to Olaparib treatment compared to control XRCC1 proficient cells (**Figure 1F, Figure 1G, Figure 1H and Figure 1I**). Interestingly, we observed a range of sensitivities to Olaparib across different cell lines. We quantified relative XRCC1 and PARP1 protein levels in matched cell lines (**Supplementary Figure S2A and S2B**). In MDA-MB-231 control XRCC1 proficient cells, the basal level of PARP1 was low. In MDA-MB-231_XRCC1_KO cells there was a higher basal level of PARP1. In MDA-MB 157 cells that have low expression of XRCC1, PARP1 level was high. In contrast, in HeLa control and XRCC1 depleted cells, we did not observe significant changes in PARP1 levels. Together the data suggest although XRCC1 depletion may result in increased PARP1 levels; it does not however, predict sensitivity to PARP inhibitor therapy.

11

We then investigated the mechanism of XRCC1 downregulation in MDA-MB-157 breast cancer cells. As shown in **Figure 1J**, the qRT-PCR analysis indicated that *XRCC1* mRNA expression was significantly low in MDA-MB-157 cells compared to MDA-MB-231 cells. Upon treatment with Azacytidine (a hypomethylating agent), *XRCC1* mRNA expression increased in MDA-MB-157 cells and was comparable to *XRCC1* mRNA expression in MDA-MB-231 cells (**Figure 1K**). Increased *XRCC1* mRNA expression was associated with increased XRCC1 protein level as shown by Western blotting (**Figure 1L**). Interestingly, Azacytidine induced XRCC1 re-expression was associated with the development of resistance to Olaparib therapy in MDA-MB-157 cells (**Figure 1M**). The data provide supportive evidence that XRCC1 expression can influence Olaparib sensitivity in cancer cells. To confirm a synthetic lethality relationship, we evaluated functional consequence of PARP inhibition in XRCC1 deficient and proficient cells.

Olaparib induces DSBs in XRCC1 deficient cells: XRCC1 deficiency leads to single-strand breaks which promote binding and activation of PARP1. Subsequent PARylation of PARP1 substrate proteins coordinates DNA repair. In addition, PARP1 autoPARylation results in its release from the DNA. PARP1 inhibitors such as Olaparib not only inhibit the catalytic activity of PARP1 but also 'trap' PARP1 at the sites of DNA damage which leads to persistent SSBs which, if unrepaired, ultimately result in accumulation of lethal DSBs in cells.

We first conducted immunofluorescence studies to monitor PARP1 and γH2AX (a marker of DSBs) levels following Olaparib treatment in XRCC1 deficient and proficient cells (**Figure 2A**). As expected basal levels of PARP1 is high in XRCC1 deficient breast cancer cells (**Figure 2A**). Upon 24 hours of Olaparib treatment, PARP1 level is sustained in XRCC1

12

deficient cells compared to proficient cells (**Figure 2A**). There was a significant increase in

γH2AX levels at 8 hours which dramatically increased at 24 hours in Olaparib treated

XRCC1 deficient cells compared to proficient cells (**Figure 2A**). We then validated by FACS

analysis. Cells were exposed to 10 μM of Olaparib for 24 hours and compared to untreated

control. As shown in **Figures 2B-2E,** Olaparib treatment significantly increased

accumulation of γH2AX positive cells in XRCC1 deficient cells [EM-C12, HeLa

XRCC1_KD silence X cells, MDA-MB-231: XRCC1_KO cells and MDA-MB-157 cells]

compared to Olaparib treated XRCC1 proficient cells and untreated controls.

Olaparib and cell cycle arrest in XRCC1 deficient cells: Accumulation of DSBs, if

unrepaired, will result in cell cycle arrest. We initially investigated cell cycle progression

upon Olaparib treatment in an asynchronous population of cells. In EM-C12 Olaparib

treatment induced G1-phase arrest (**Figure 2F**) (see **Supplementary Table S5** for

quantification). In HeLa XRCC1_KD silence X cells, and MDA-MB-157 cells, Olaparib

treatment induced S-phase arrest (**Figures 2G-2H)** (see **Supplementary Table S5** for

quantification)**.** However, in MDA-MB-231: XRCC1_KO cells, Olaparib treatment induced

G2/M-phase arrest compared to control cells (**Figures 2I)** (see **Supplementary Table S5** for

quantification). We then synchronized cells by serum starvation for 16 hours. As expected, all

cell lines arrested at G1-phase (**Figure 3A**). The cell lines were then released in serum-

containing media with or without Olaparib treatment. At 24 hours, similar to asynchronous

population, we observed substantial accumulation of cells in S- phase upon Olaparib

treatment in HeLa XRCC1_KD silence X cells (**Figure 3A, 3B**) and MDA-MB-157 cells

(**Figure 3A, 3C**). In MDA-MB-231: XRCC1_KO cells, G2/M arrest was evident and

substantial compared to Olaparib treated control and untreated cells (**Figure 3A, 3C**).

13

The data suggest that the cell cycle response in various cell lines may be influenced by genetic backgrounds including p53 status. We profiled p53 (**Supplementary Figure S2C**) for mutant p53, phosphorylated forms of p53 at Ser 46, Ser 20 and Ser 392 and acetylated form of p53 at Lys 382. As shown in Supplementary Figure S2C, HeLa cells are wild type for p53. MDA-MB-231 and MDA-MB-157 cells harbour activating p53 mutation. Nutlin-3, a potent inhibitor of MDM2-p53 interaction can activate p53 mediated pathway in cells (16). To determine if the cell cycle arrest observed in Olaparib treated XRCC1 deficient cells may be influenced by p53, we monitored cell cycle progression in cells treated either with Nutlin alone or with Nutlin / Olaparib combination. Olaparib alone resulted in S-phase arrest in MDA-MB-157 cells (**Figure 3A)** but Olaparib/Nutlin combination lead to G2/M arrest in MDA-MB-157 cells (**Figure 3D**). Interestingly, in MDA-MB-231_XRCC1 KO cells, Olaparib alone resulted in G2/M arrest (**Figure 3C)** but Olaparib/Nutlin combination lead to S-phase arrest in MDA-MB-231_XRCC1 KO cells. (**Figure 3D**). In HeLa cells, Olaparib treatment resulted in S-phase arrest (**Figure 2G**) and with Olaparib/Nutlin combination the cells remain arrested in S-phase (**Supplementary Figure S2D**). When p53 was depleted using siRNA in HeLa cells, Olaparib treatment resulted in G2/M arrest (**Supplementary Figure S2D**). Taken together, the data provide evidence that cell cycle response to Olaparib treatment in XRCC1 deficient cells is complex and p53 mediated pathway may not be significantly involved in the cell cycle response. We then evaluated regulators of cell cycle progression by western blotting in Olaparib treated and untreated cells (**Supplementary Figure S2E**). In S-phase arrested HeLa XRCC1_KD silence X cells, we observed an increase in the level of Cyclin E1 and a reduction in the level of p21 after Olaparib treatment. In addition, Olaparib treatment also reduced the level of p21 in MDA-MB-157 cells leading onto S-phase arrest. In G2/M arrested MDA-MB-231: XRCC1_KO cells, we observed an increase in the level of p-Cyclin B1 upon Olaparib treatment. Together the data illustrates a

14

complex cell cycle regulator response following Olaparib treatment in various XRCC1 deficient cells.

Olaparib and apoptosis in XRCC1 deficient cells: SSBs/DSBs, if unrepaired will lead to cell cycle arrest and eventually induce apoptosis in cells. Accordingly, we observed significant induction of apoptosis at 48 hours in Olaparib treated EM-C12, HeLa XRCC1_KD silence X cells, MDA-MB-157 and MDA-MB-231: XRCC1_KO cells compared to control and untreated cells (**Figure3E-3H**). To recapitulate an *in vivo* system, we then generated 3D-spheroids of MDA-MB-231 control, MDA-MB-231 XRCC1 KO, and MDA-MB-157 cells. Similar to control cells, untreated XRCC1 KO cells retain spheroid forming capacity. However, upon Olaparib treatment in XRCC1 KO cells, there was not only a reduction in spheroid size (**Figure 3I, 3J, and 3K**) but also an accumulation of apoptotic cells (**Figure 3L**).

Olaparib as a chemoprevention strategy in XRCC1 deficient breast ductal carcinoma in situ (DCIS): Ductal carcinoma in situ (DCIS), a pre-invasive breast cancer, continues to increase in incidence (17). The main aim of treatment is to prevent DCIS from progressing to invasive cancer. Accordingly, surgery (mastectomy or wide local excision), with or without adjuvant radiotherapy are the main treatment modalities. However, personalization of DCIS therapy is an area of unmet need. For example, it is likely that a subset of low-grade DCIS may never progress to invasive cancer. In a subset of high grade disease, despite surgery and adjuvant radiotherapy may still recur. Therefore, development of biomarkers of aggressive phenotype is highly desirable. Emerging data suggest that aggressive DCIS may result from the accumulation of somatic mutations. We hypothesised that impaired DNA repair capacity due to XRCC1 deficiency may be a key contributor to the development of high-grade DCIS.

15

We evaluated XRCC1 expression (**Figure 4A**) in a cohort of 776 patients with DCIS diagnosed between 1987 and 2012 at Nottingham University Hospitals (demographics summarized in **Supplementary Table S6**). Whereas normal breast tissues have high levels of XRCC1 expression, the XRCC1 level substantially reduced in DCIS and invasive breast cancers (**Figure 4B**). The data provide clinical evidence that loss of   XRCC1 expression (observed in 54.3% of DCIS) is an early event during breast cancer pathogenesis. In addition, high-grade DCIS (p=0.05), ER negativity (p=0.015) and older age (p=0.048) were also more common in patients with XRCC1 deficient DCIS (**Supplementary Table S7**). Importantly, the local recurrence-free interval was significantly reduced in patients with XRCC1 deficient DCIS compared XRCC1 proficient DCIS (p=0.001) (**Figure 4C**). The clinical data, therefore, provide evidence that low XRCC1 expression is a biomarker of aggressive DCIS. To evaluate the potential of Olaparib as a chemoprevention strategy in XRCC1 deficient DCIS we proceeded to pre-clinical investigations.

MCF10DCIS breast cancer cell line was previously derived from a xenograft originating from premalignant MCF10AT cells injected into SCID mice (18). Injection of the MCF10DCIS cells into SCID mice results in a predominantly comedo ductal carcinoma in situ phenotype (18, 19). We show robust levels of XRCC1 expression in MCF10DCIS cells (**Figure 4D**). In contrast to MDA-MB-231, MCF10DCIS cells are as expected non-invasive, a phenotype similar to MCF10A non-cancerous epithelial cells (**Figure 4E,**). We then proceeded to generate MCF10DCIS_XRCC1_KO using CRISPR/Cas-9 system (**Figure 4F**). XRCC1 _KO was associated with increased PARP1 levels compared to control cells (**Figure 4G**). In contrast to control cells, MCF10DCIS_XRCC1_KO cells not only acquired an invasive phenotype (**Figure 4H, 4I**) but was also associated with up-regulation of several genes involved in epithelial-mesenchymal transition (EMT) (**Figure 4I**)

16

(**Supplementary Table S8**). In addition, spindle-shaped cells with elongated cellular processes and diminished cell-to-cell contacts were more evident in MCF10DCIS_XRCC1_KO cells (**Figure 4I**). Importantly, MCF10DCIS _XRCC1 _KO cells were very sensitive to Olaparib treatment (**Figure 4J**) compared to control cells. Increased Olaparib sensitivity was associated with accumulation of γH2AX positive cells (**Figure 4K**), G2/M cell cycle arrest (**Figure 4L**) and apoptosis (**Figure 4M**). To recapitulate an *in vivo* system, we then generated 3D-spheroids of MCF10DCIS _XRCC1 _KO cells and MCF10DCIS control cells. Similar to control cells, untreated MCF10DCIS _XRCC1_KO cells retain spheroid forming capacity (**Figure 4N**). However, Olaparib treatment strikingly reduced viability and spheroid forming ability (**Figure 4N**). Taken together the data provide evidence that XRCC1 deficient human DCIS are aggressive and Olaparib is synthetically lethal in XRCC1 deficient MCF10DCIS cells.

Evaluation of Niraparib and Talazoparib sensitivity in XRCC1 deficient cells: The data presented thus far suggest that the hypersensitivity observed in XRCC1 deficient cells may be influenced by the effectiveness of the Olaparib to "trap" PARP proteins. However, to validate this hypothesis we evaluated other clinically relevant PARP inhibitors including Niraparib and Talazoparib that have increased ability to "trap" PARP. Talazoparib is about 100 more potent than Niraparib for PARP trapping. Niraparib, in turn, traps PARP more potently than Olaparib (1). As expected, XRCC1 deficient cells are sensitive to Niraparib (**Supplementary Figure 2F**) and to Talazoparib (**Figure 5A**) compared to control cells. LD50 analysis (**Supplementary Table S9**) revealed that at doses tested, Niraparib was five times more potent than Olaparib. Talazoparib was twenty times more potent than Olaparib (**Supplementary Table S9**). Given the impressive hypersensitivity to Talazoparib, we then conducted detailed functional studies. Confocal studies revealed that nuclear PARP

17

accumulation was evident within 4 hours of Talazoparib treatment, which substantially increased at 16 hours and persisted at 24 hours in XRCC1 deficient cells (Figure 5B and 5C). γH2AX accumulation was also evident at 8 hours, 16 hours and 24 hours. We confirmed DSB accumulation using γH2AX FACS (Figure 5D). Furthermore increased sensitivity to Talazoparib was associated with G2/M cell cycle arrest (Figure 5E) and increased apoptosis (Figure 5F). Importantly in 3D- spheroids experiments, we observed that XRCC1 deficient 3D- spheroids were sensitivity to Talazoparib, as evidenced by the substantial reduction in spheroid size as well as increased apoptotic cells (Figure 5G, 5H and 5I). Taken together, the data provide additional validation that PARP 'trapping' is likely to contribute to the observed PARP inhibitor sensitivity in XRCC1 deficient cells.

18

DISCUSSIONS

XRCC1 is a key scaffolding protein intimately involved in BER, SSBR, and alt-NHEJ (3, 4, 7). XRCC1 loss promotes genomic instability (3, 4). XRCC1 interacts with PARP1 during DNA repair (5, 6). A previous high throughput siRNA screen identified XRCC1 as a synthetic lethality partner for PARP inhibition (20). Pre-clinically, Xrcc1 [-/-] mouse embryonic fibroblasts were shown to be hypersensitive to PARP inhibitor treatment compared to Xrcc1 [+/+] mouse embryonic fibroblasts (21) suggesting that this approach could have clinical relevance in human tumours including in breast cancers.

We have previously demonstrated that XRCC1 deficiency is linked to aggressive breast tumours including in triple negative breast cancers (TNBC) (15). In the current study, we not only show that high PARP1 levels in XRCC1 deficient tumours is associated with aggressive breast cancer but also provide compelling evidence that PARP1 targeting is suitable for synthetic lethality application. A model for XRCC1 directed synthetic lethality has been proposed previously (21). PARP1 binds to DNA repair intermediates such as single-strand breaks and gets activated which in turn leads to the synthesis of PAR (poly-ADP-ribose) polymers. PARP1 auto-PARylation recruits other BER factors (including XRCC1) at sites of DNA damage resulting in efficient DNA repair. Inhibition of PARP1 catalytic activity (by inhibitor) prevents auto-PARylation, impairs BER recruitment and stabilises binding of PARP1 to DNA intermediate. DNA-bound immobilised PARP-1 disrupts replication fork progression, leads to double-strand break (DSB) accumulation and DSB-mediated apoptosis. In XRCC1 deficient cells with increased SSB accumulation, PARP inhibition mediated accumulation of DSB is more pronounced compared to XRCC1 proficient cells leading to synthetic lethality (21). Accordingly, in XRCC1 deficient breast cancer cells treated with

19

Olaparib, we observed nuclear PARP accumulation, increased γH2AX foci in the nucleus, cell cycle arrest and induction of apoptosis. Interestingly, we also observed cytoplasmic PARP and cytoplasmic γH2AX in Olaparib treated XRCC1 deficient cells. Although majority of cellular PARP activity is localized to the nucleus, the cytoplasm has been shown previously to have PARP activity (22) including in the mitochondria (23). Besides DNA repair, PARP has recognised roles in mitochondrial homeostasis, oxidative stress and cell death (23). Similarly, cytoplasmic γH2AX has also been reported (24). Jung et al have shown that Tropomyosin- related kinase A mediated cytoplasmic γH2AX via JNK signalling may have a role in apoptosis (24). We therefore speculate that the observed cytoplasmic PARP and γH2AX may reflect their roles in apoptosis in Olaparib treated XRCC1 deficient cells. Taken together the data provide the first translational evidence that PARP1 targeting (e.g. Olaparib) may have a wider clinical application in XRCC1 deficient sporadic breast cancers. Interestingly, the cell cycle pattern observed in MDA-MB-231 control cells treated with Olaparib was unexpected. A previous study (25) showed that PARP-1 promoted cell proliferation by inhibiting Sp1 signaling pathway. PARP inhibitors significantly inhibited proliferation of hepatoma cells and induced G0/G1 cell cycle arrest in hepatoma cells. Inhibition of PARP-1 enhanced the expression of Sp1-mediated checkpoint proteins including p21 resulting in G0/G1 cell cycle arrest in that study. We observed a similar phenotype in MDA-MB-231 control cells where Olaparib treatment induced G1 cell cycle arrest (Figure 3C) and induction of p21 expression (**Supplementary Figure S2E**).

XRCC1 deficiency promotes aggressive invasive cancerous phenotypes. To test whether XRCC1 also influences clinical outcomes in pre-invasive DCIS, we investigated XRCC1 expression in a large clinical cohort of human breast DCIS. In contrast to normal breast tissue that had a high XRCC1 expression, there was a dramatic reduction in XRCC1 levels in DCIS

20

particularly those with high grade or ER-negative. Although the mechanism of XRCC1 downregulation in DCIS is currently unknown, the data suggest that loss of DNA repair could be an early event in human breast cancer pathogenesis. More importantly, we also observed that XRCC1 deficiency was also linked to increased risk of local recurrence. In a preclinical MCF10DCIS model, we show that XRCC1 KO dramatically increased invasion associated with up-regulation of markers of epithelial-mesenchymal-transition (EMT). Whether XRCC1 is directly or indirectly involved in up-regulation of several genes involved in EMT is unknown but the data shown here would concur with previous studies in melanoma (26) and clear cell renal cancer (27) cells where XRCC1 depletion was also shown to promote invasion. A novel observation in the current study is that MCF10DCIS_ XRCC1_ KO cells are extremely sensitive to Olaparib therapy. Interestingly, Olaparib maintenance almost completely abolished the 3D-spheroid forming ability of MCF10DCIS_XRCC1_KO cells compared to controls. The data provides the first promising evidence that Olaparib may have a role in chemoprevention of XRCC1 deficient DCIS.

Impaired DNA repair drives mutagenicity, which can increase neo-antigen load and immunogenicity. Whether PARP targeting in combination with immune checkpoint inhibitor can improve therapeutic efficacy is currently an area of intense clinical investigation. However, biomarkers that could predict such an approach are currently unknown. We recently investigated XRCC1 and T-cell infiltration in invasive breast cancers (13). Tumours that expressed low XRCC1 were associated with high CD8^{+} tumour-infiltrating lymphocyte (TILs) counts, aggressive phenotype and reduced survival. Importantly, PD-1^{+} or PD-L1^{+} breast cancers with low XRCC1 were linked to aggressive cancers and reduced survival including in ER[−] breast cancers (13). As immune microenvironment (including PD-L1[+] TILs infiltration) in DCIS can influence aggressive phenotypes (28, 29), we propose that PARP1

21

targeting may be a promising personalized approach either alone or in combination with

immune checkpoint inhibitors in XRCC1 deficient invasive cancers and in pre-invasive

DCIS.

22

REFERENCES

1.   Lord CJ,Ashworth A. PARP inhibitors: Synthetic lethality in the clinic. Science **2017**;355:1152-8

2.   Lord CJ,Ashworth A. BRCAness revisited. Nat Rev Cancer **2016**;16:110-20

3.   Caldecott KW. XRCC1 and DNA strand break repair. DNA Repair (Amst) **2003**;2:955-69

4.   London RE. The structural basis of XRCC1-mediated DNA repair. DNA Repair (Amst) **2015**;30:90-103

5.   El-Khamisy SF, Masutani M, Suzuki H,Caldecott KW. A requirement for PARP-1 for the assembly or stability of XRCC1 nuclear foci at sites of oxidative DNA damage. Nucleic Acids Res **2003**;31:5526-33

6.   Masson M, Niedergang C, Schreiber V, Muller S, Menissier-de Murcia J,de Murcia G. XRCC1 is specifically associated with poly(ADP-ribose) polymerase and negatively regulates its activity following DNA damage. Mol Cell Biol **1998**;18:3563-71

7.   Deriano L,Roth DB. Modernizing the nonhomologous end-joining repertoire: alternative and classical NHEJ share the stage. Annu Rev Genet **2013**;47:433-55

8.   Moser J, Kool H, Giakzidis I, Caldecott K, Mullenders LH,Fousteri MI. Sealing of chromosomal DNA nicks during nucleotide excision repair requires XRCC1 and DNA ligase III alpha in a cell-cycle-specific manner. Mol Cell **2007**;27:311-23

9.   Hoch NC, Hanzlikova H, Rulten SL, Tetreault M, Komulainen E, Ju L, et al. XRCC1 mutation is associated with PARP1 hyperactivation and cerebellar ataxia. Nature **2017**;541:87-91

10.   O'Connor E, Vandrovcova J, Bugiardini E, Chelban V, Manole A, Davagnanam I, et al. Mutations in XRCC1 cause cerebellar ataxia and peripheral neuropathy. J Neurol Neurosurg Psychiatry **2018**

11.   Abdel-Fatah TM, Arora A, Moseley PM, Perry C, Rakha EA, Green AR, et al. DNA repair prognostic index modelling reveals an essential role for base excision repair in influencing clinical outcomes in ER negative and triple negative breast cancers. Oncotarget **2015**;6:21964-78

12.   Abdel-Fatah TM, Perry C, Arora A, Thompson N, Doherty R, Moseley PM, et al. Is there a role for base excision repair in estrogen/estrogen receptor-driven breast cancers? Antioxid Redox Signal **2014**;21:2262-8

13.   Green AR, Aleskandarany MA, Ali R, Hodgson EG, Atabani S, De Souza K, et al. Clinical Impact of Tumor DNA Repair Expression and T-cell Infiltration in Breast Cancers. Cancer Immunol Res **2017**;5:292-9

14.   Green AR, Caracappa D, Benhasouna AA, Alshareeda A, Nolan CC, Macmillan RD, et al. Biological and clinical significance of PARP1 protein expression in breast cancer. Breast Cancer Res Treat **2015**;149:353-62

15.   Sultana R, Abdel-Fatah T, Abbotts R, Hawkes C, Albarakati N, Seedhouse C, et al. Targeting XRCC1 deficiency in breast cancer for personalized therapy. Cancer Res **2013**;73:1621-34

16.   Burgess A, Chia KM, Haupt S, Thomas D, Haupt Y,Lim E. Clinical Overview of MDM2/X-Targeted Therapies. Front Oncol **2016**;6:7

17.   Barnes NL, Ooi JL, Yarnold JR,Bundred NJ. Ductal carcinoma in situ of the breast. BMJ **2012**;344:e797

18.   Band V,Sager R. Distinctive traits of normal and tumor-derived human mammary epithelial cells expressed in a medium that supports long-term growth of both cell types. Proc Natl Acad Sci U S A **1989**;86:1249-53

23

19. Miller FR, Santner SJ, Tait L,Dawson PJ. MCF10DCIS.com xenograft model of human comedo ductal carcinoma in situ. J Natl Cancer Inst **2000**;92:1185-6

20. Lord CJ, McDonald S, Swift S, Turner NC,Ashworth A. A high-throughput RNA interference screen for DNA repair determinants of PARP inhibitor sensitivity. DNA Repair (Amst) **2008**;7:2010-9

21. Horton JK, Stefanick DF, Prasad R, Gassman NR, Kedar PS,Wilson SH. Base excision repair defects invoke hypersensitivity to PARP inhibition. Mol Cancer Res **2014**;12:1128-39

22. Vyas S, Chesarone-Cataldo M, Todorova T, Huang YH,Chang P. A systematic analysis of the PARP protein family identifies new functions critical for cell physiology. Nat Commun **2013**;4:2240

23. Bai P. Biology of Poly(ADP-Ribose) Polymerases: The Factotums of Cell Maintenance. Mol Cell **2015**;58:947-58

24. Jung EJ, Kim CW,Kim DR. Cytosolic accumulation of gammaH2AX is associated with tropomyosin-related kinase A-induced cell death in U2OS cells. Exp Mol Med **2008**;40:276-85

25. Yang L, Huang K, Li X, Du M, Kang X, Luo X, et al. Identification of poly(ADP-ribose) polymerase-1 as a cell cycle regulator through modulating Sp1 mediated transcription in human hepatoma cells. PLoS One **2013**;8:e82872

26. Bhandaru M, Martinka M, Li G,Rotte A. Loss of XRCC1 confers a metastatic phenotype to melanoma cells and is associated with poor survival in patients with melanoma. Pigment Cell Melanoma Res **2014**;27:366-75

27. Liu QH, Wang Y, Yong HM, Hou PF, Pan J, Bai J, et al. XRCC1 serves as a potential prognostic indicator for clear cell renal cell carcinoma and inhibits its invasion and metastasis through suppressing MMP-2 and MMP-9. Oncotarget **2017**;8:109382-92

28. Hendry S, Pang JB, Byrne DJ, Lakhani SR, Cummings MC, Campbell IG, et al. Relationship of the Breast Ductal Carcinoma In Situ Immune Microenvironment with Clinicopathological and Genetic Features. Clin Cancer Res **2017**;23:5210-7

29. Thompson E, Taube JM, Elwood H, Sharma R, Meeker A, Warzecha HN, et al. The immune microenvironment of breast ductal carcinoma in situ. Mod Pathol **2016**;29:249-58

24

Figure Legends

Figure 1: (A). Immunohistochemical expression of XRCC1 and PARP1 in breast cancers. XRCC1 & PARP1 co-expression and Kaplan-Meier curve for BCSS (breast cancer specific survival) in TNBC (whole cohort) (B), TNBCs that received no chemotherapy (C) and TNBCs treated with chemotherapy (D). (E) XRCC1 expression in various cell lines. Clonogenic cell survival in Olaparib treated cells [(F) CHO9 and EMC12 cells, (G) HeLa control and HeLa XRCC1 deficient cells, (H) 231 control and 157 cells and (I) 231 and 231:XRCC1_KO cells]. *XRCC1* mRNA levels in 231 and 157 cells (J and K). (L) XRCC1 expression in 157 cells treated with Azacytidine (1.5µM). (M) Cell proliferation assay in cells treated with Olaparib and Azacytidine compared Olaparib alone. All figures are representative of three or more independent experiments.

Figure 2: (A) Immunofluorescence staining for PARP1 and γH2AX in 231control, 231:XRCC1_KO and 157 cells treated with Olaparib (10µM) are shown here. Quantification of γH2AX positive cells by flow cytometry in: CHO9 & EMC12 cells (B), HeLa control & HeLa XRCC1 deficient cells (C), 231 control & 157 cells (D) and 231 control & 231: XRCC1_KO cells (E). Cell cycle analysis by flow cytometry in XRCC1 proficient and deficient cells treated with Olaparib (10 µM) in CHO9 & EMC12 cells (F), HeLa control & HeLa XRCC1 deficient cells (G), 231 control & 157 cells (H) and 231 control & 231:XRCC1_KO cells (I).All cell lines were plated overnight and treated with Olaparib(10 µM) for 24 hours before harvesting for flow cytometry experiments as described in methods. All figures are representative of three or more independent experiments.

Figure 3: (A) Cell cycle synchronization in various cell lines. FACS analysis in synchronized HeLa control & HeLa XRCC1 deficient cells treated with Olaparib (10 µM) (B), 231 control & 231:XRCC1_KO and 157 cells (C). (D) Cell cycle analysis in

25

synchronized 231 control, 231:XRCC1_KO and 157 treated with Nutlin 3a (10 µM) and/or

Olaparib (10 µM) . Annexin V analysis by flow cytometry in: CHO9 & EMC12 cells (E),

HeLa control & HeLa XRCC1 deficient cells (F), 231 control & 157 cells (G), and 231

control & 231:XRCC1_KO cells (H). All cell lines were plated overnight and treated with

Olaparib (10 µM) for 24 hours before harvesting for flow cytometry experiments as described

in methods. (I) Representative photo micrographic images of 3D spheres of 231 control,

231:XRCC1_KO and 157 cells untreated or treated with Olaparib (10 µM). Measurement of

spheres surface area in square pixels for :231 control untreated or treated with Olaparib (10

µM). (J) and 231:XRCC1_KO as well as 157 untreated or treated with Olaparib (10 µM).

(K). (L) Quantification of viable and dead cells is shown here. All figures are representative

of three or more independent experiments.

Figure 4: (A) XRCC1 expression in DCIS. (B) Box plot of XRCC1 expression in normal,

DCIS and invasive tumours. (C) Kaplan Meier curve showing association between XRCC1

and local recurrence. (D) XRCC1 expression in 231, MCF-7, MCF10DCIS and MCF10A cell

lines. (E) Photo micrographic images of cell invasion in MCF10A, MCF10DCIS and 231

cells as well as quantification data. (F) XRCC1 expression in MCF10DCIS_KO cells or

controls. (G) PARP1 expression in MCF10DCIS_KO cells or controls. (H) Photo

micrographic   images   of   cell   migration   in   MCF10DCIS   control   and

MCF10DCIS_XRCC1_KO as well as quantification data.   (I) Cell morphology of

MCF10DCIS_XRCC1_KO & MCF10DCIS control cells as well as EMT gene expression in

MCF10DCIS control and XRCC1_KO cells using RT^2-PCR profiler is shown here. (J)

Olaparib sensitivity in MCF10DCIS control and MCF10DCIS_XRCC1_KO cells. (K)

Quantification of γH2AX positive cells in MCF10DCIS control and XRCC1_KO cells

treated with Olaparib (10 µM) for 24 hrs. (L) Cell cycle analysis in MCF10DCIS control and

MCF10DCIS_XRCC1_KO   cells.   (M)   Annexin   V   analysis   by   flow   cytometry   in

26

MCF10DCIS control and MCF10DCIS_XRCC1_KO cells. All cells were plated overnight and treated with Olaparib(10 µM) for 24 hours before harvesting for flow cytometry experiments as described in methods. (N) Photo micrographic images of Olaparib (10 µM) treated MCF10 DCIS 3D spheres (see methods for details). All figures are representative of three or more independent experiments. DCIS= ductal carcinoma in situ, IBC= invasive breast cancer.

Figure 5: (A) Clonogenic cell survival in Talazoparib treated cells. **(B)** Immunofluorescence staining for PARP1 and γH2AX in 231control, 231:XRCC1_KO cells untreated or treated with Talazoparib (5µM). (C) Quantification of PARP and γH2AX nuclear fluorescence. (D) Quantification of γH2AX positive cells by flow cytometry in Talazoparib (5µM) treated cells. (E) Cell cycle analysis by flow cytometry is shown here. (F) Quantification of apoptotic cells. All cell lines were plated overnight and treated with Talazoparib (5 µM) for 24 hours before harvesting for flow cytometry experiments as described in methods. (G) Photo micrographic images of Talazoparib (5µM) treated 3D-spheroids. (H) Quantification of spheres surface area by image j software. (I) Quantification of spheroids cell viability by flow cytometry.

27

Figure 1

Figure 2

Figure 3

Figure 4

Figure 5
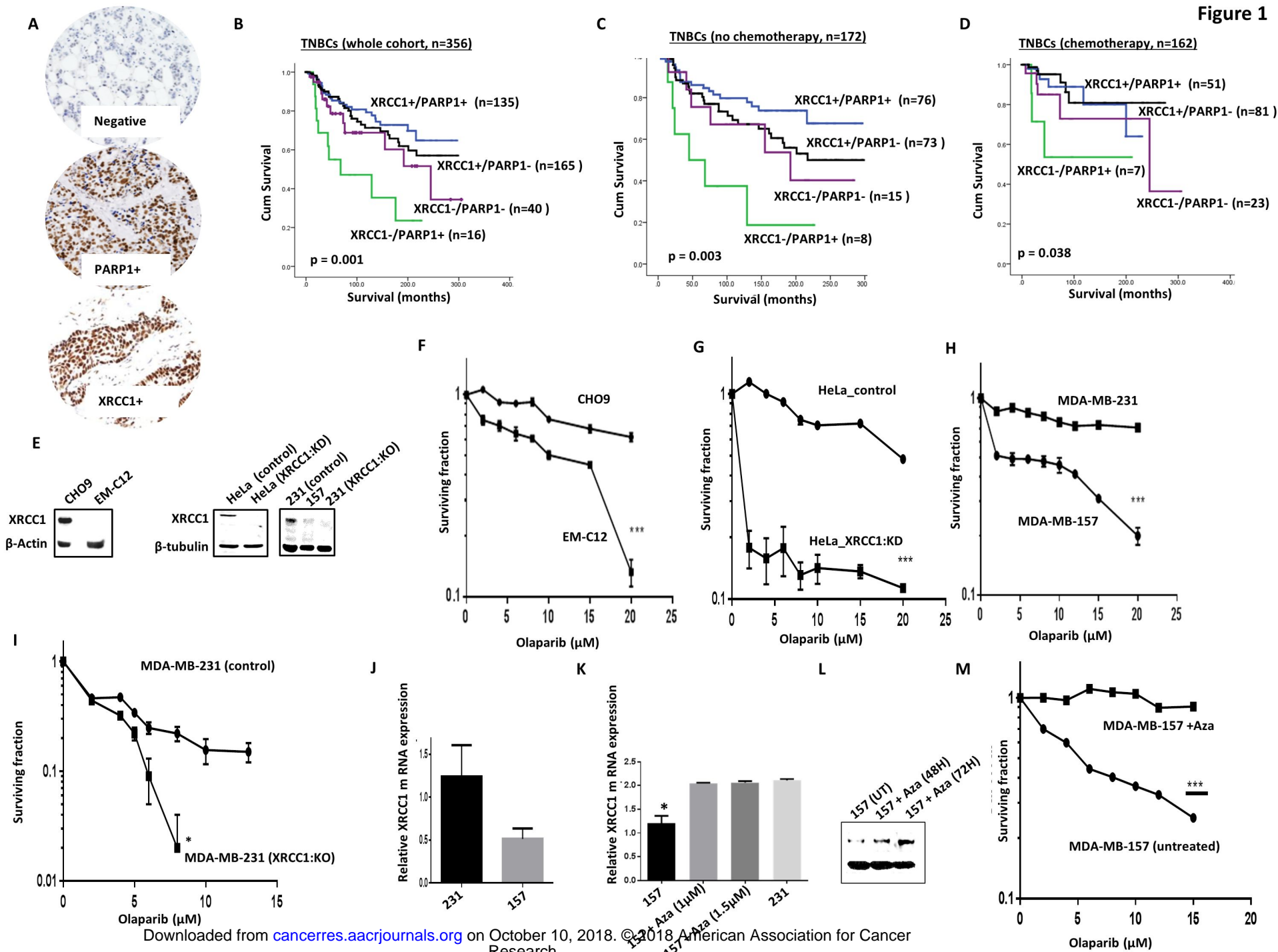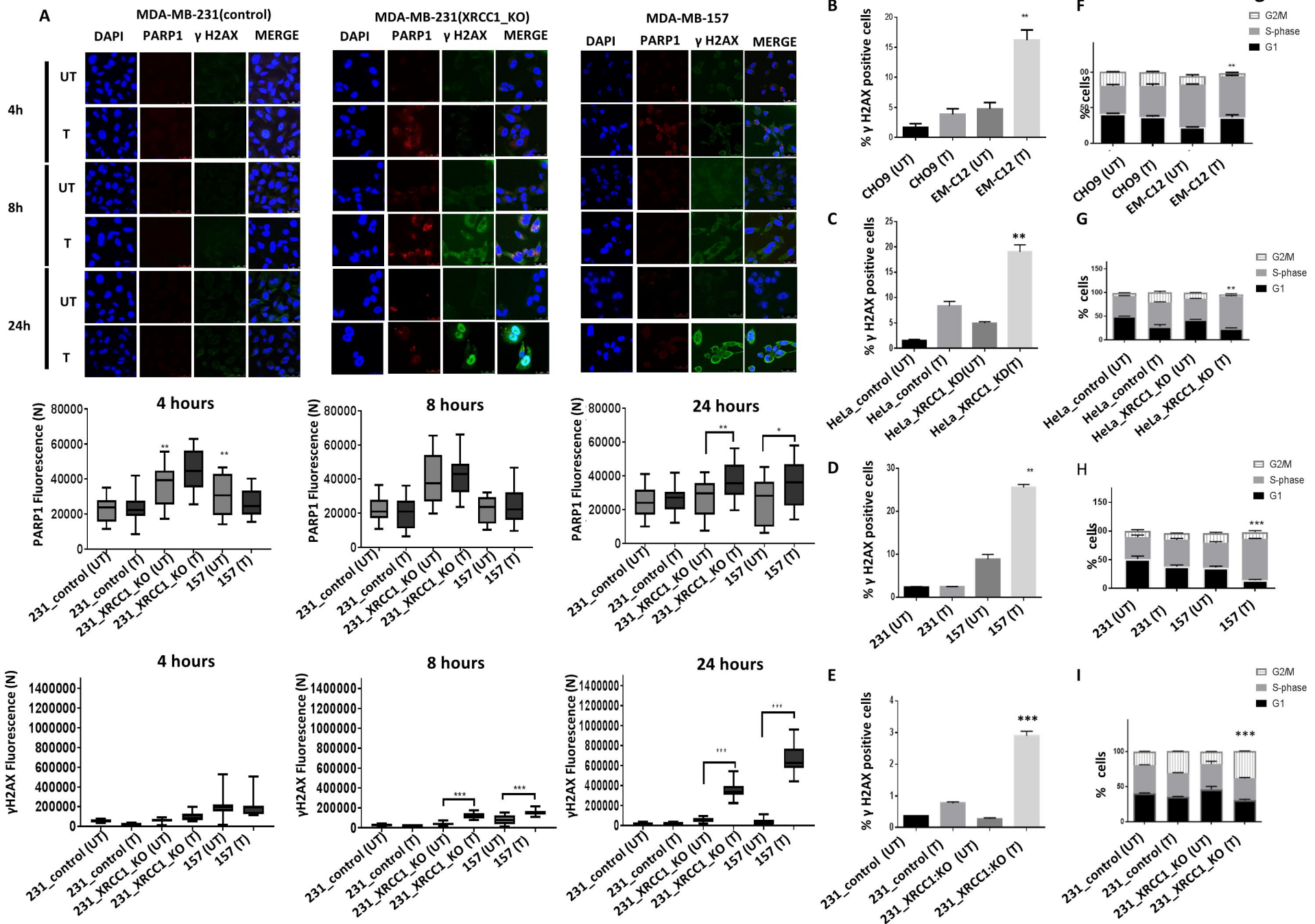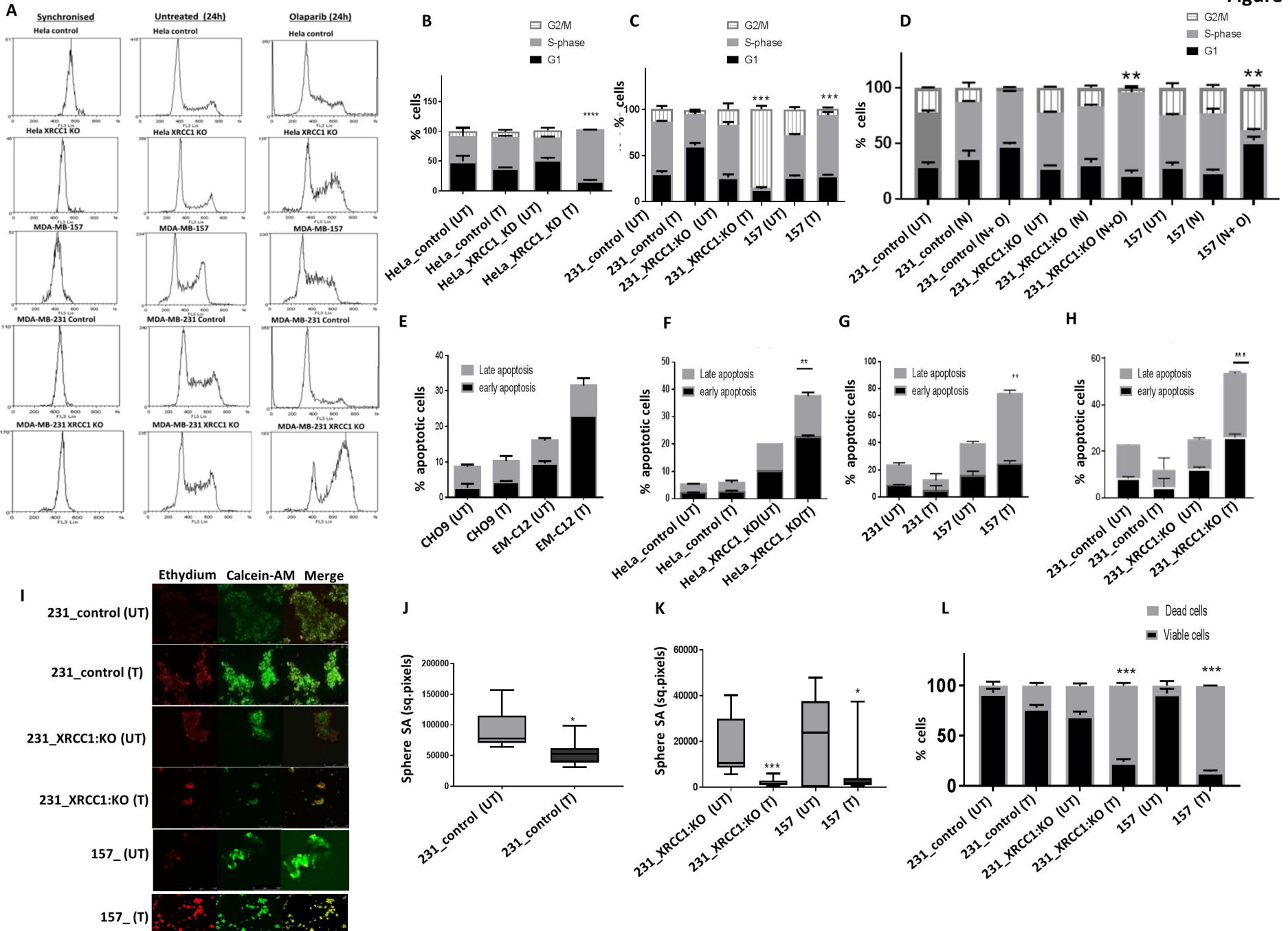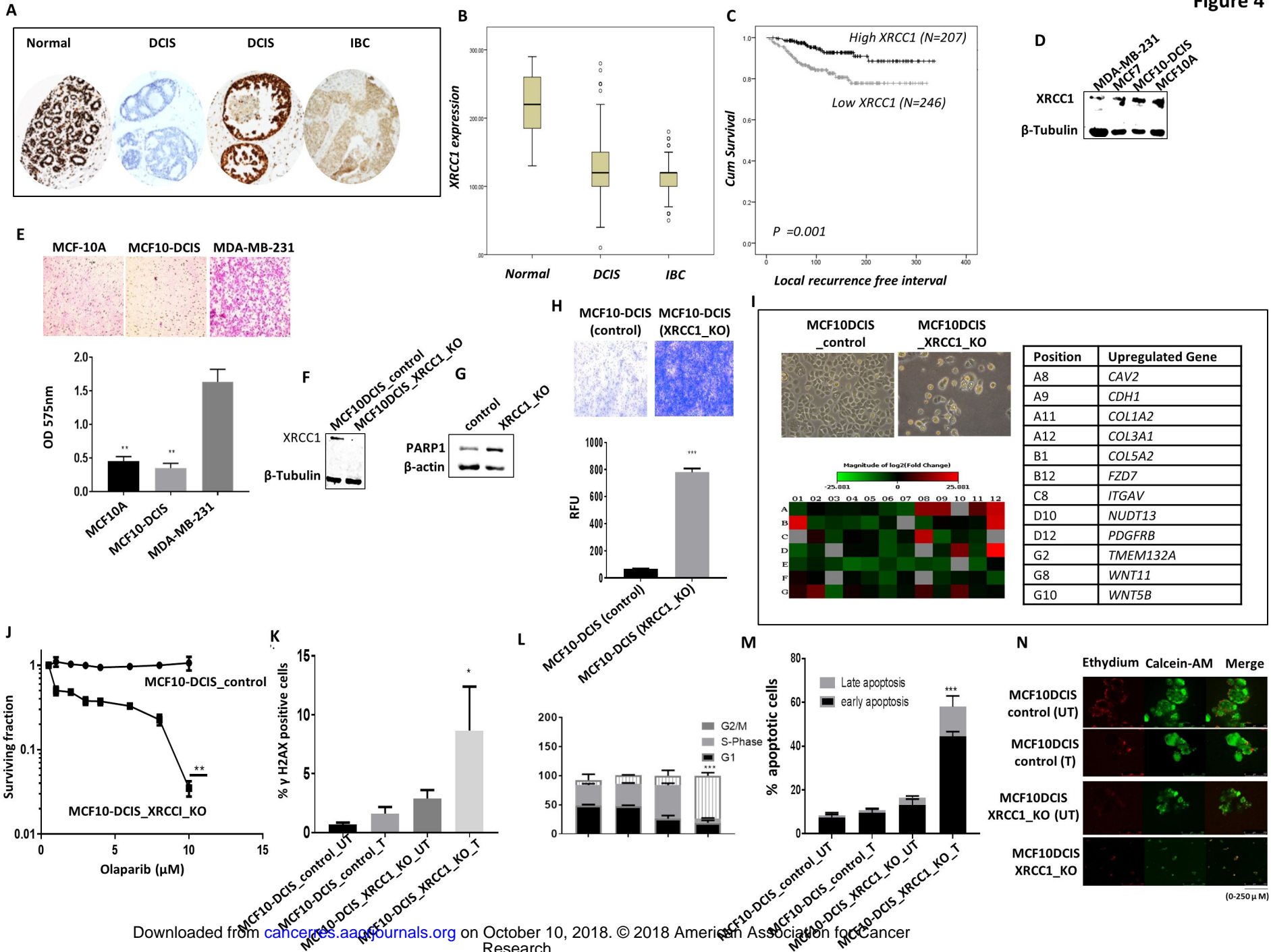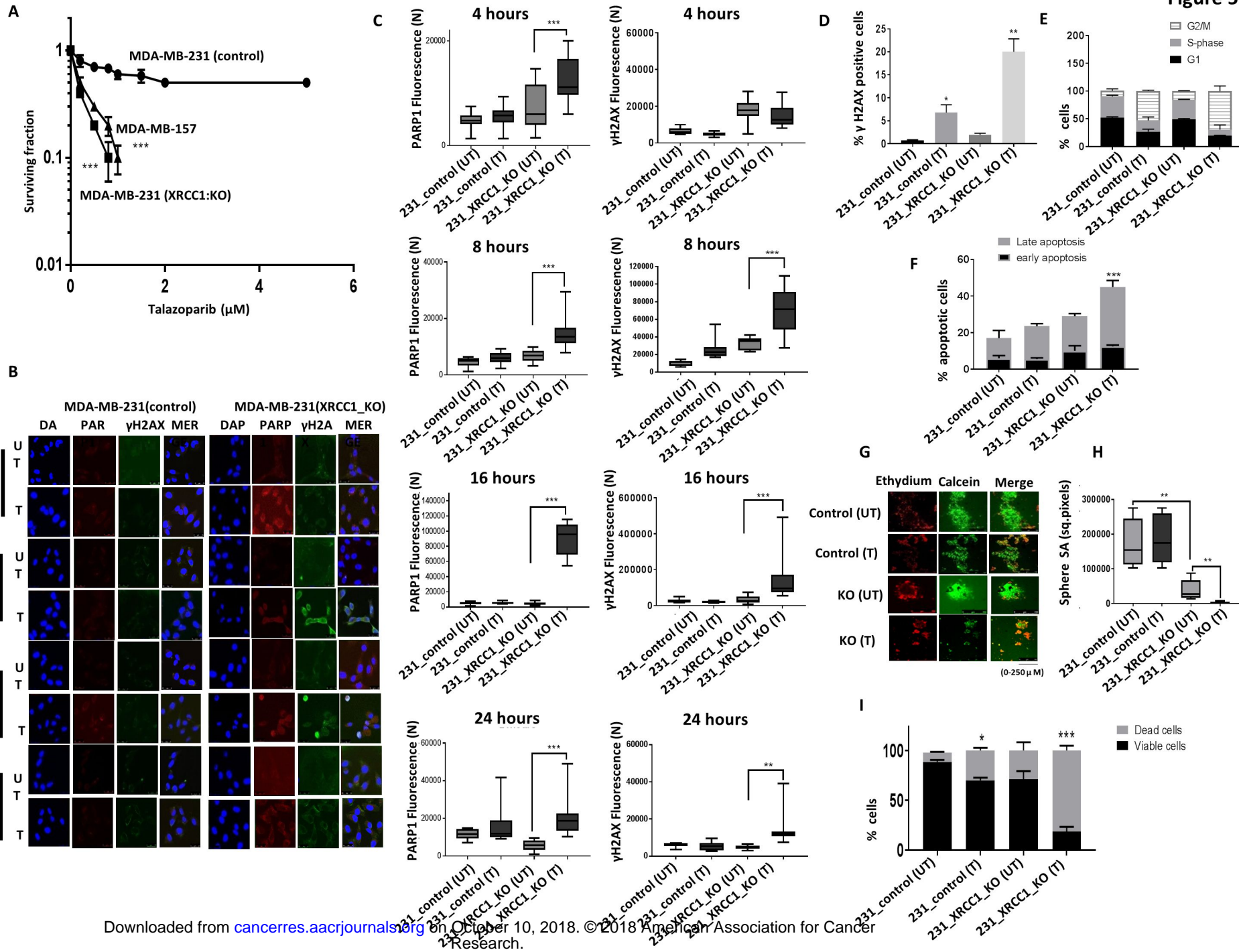
Cancer Research

The Journal of Cancer Research (1916–1930) | The American Journal of Cancer (1931–1940)

Targeting PARP1 in XRCC1 deficient sporadic invasive breast cancer or pre-invasive ductal carcinoma in situ induces synthetic lethality and chemoprevention

Reem Ali, Abdulbaqi Al-kawaz, Michael S Toss, et al.

Updated version	Access the most recent version of this article at: doi:10.1158/0008-5472.CAN-18-0633
Supplementary Material	Access the most recent supplemental material at: http://cancerres.aacrjournals.org/content/suppl/2018/10/06/0008-5472.CAN-18-0633.DC1
Author Manuscript	Author manuscripts have been peer reviewed and accepted for publication but have not yet been edited.

E-mail alerts	Sign up to receive free email-alerts related to this article or journal.
Reprints and Subscriptions	To order reprints of this article or to subscribe to the journal, contact the AACR Publications Department at pubs@aacr.org.
Permissions	To request permission to re-use all or part of this article, use this link http://cancerres.aacrjournals.org/content/early/2018/10/06/0008-5472.CAN-18-0633. Click on "Request Permissions" which will take you to the Copyright Clearance Center's (CCC) Rightslink site.

SUPPLEMENTARY MATERIALS AND METHODS

MATERIALS AND METHODS

Compounds and reagents: Olaparib (AZD2281) was kindly provided by AstraZeneca Pharmaceuticals. Talazoparib and Niraparib were purchased from Selleckchem, UK. The antibodies used in the current study are as follows; XRCC1 antibody clone (33-2-5) (Thermofisher, UK), CyclinE1 (ab33911), p-CyclinB1 (ab55184), p21 (ab7960), Mutant p53 antibody (ab32049), (Abcam,UK) and p53 antibody panel (ab219089). Histone H2AX phosphorylated at Ser^{139} (γH2AX; 05–636; Millipore, UK) and PARP1 antibody (Cell signalling, USA). Azacytidine and Nutlin 3a were purchased from Sigma, UK. Pre-validated p53 siRNA was purchased from Invitrogen. Lipofecamine3000 reagent, Calcein AM and Ethidium homodimer -1were purchased from Thermofisher, UK.

Generation of XRCC1 knockouts using CRISPR/Cas-9 system: MDA-MB-231 and MCF-10DCIS were transfected with oligonucleotides carrying gRNA silencing XRCC1cloned in a Plv-U6g-EPCG plasmid (Sigma, UK).Briefly, cells were seeded at 50- 60 % confluency in 6 well plates overnight. Cells were transfected with 2-3 µg of DNA using Lipofectamine 3000(Invitrogen, UK) in an Opti-MEM medium. Puromycin was used as a selection marker for 14 days. MDA-MB-231 was selected in 10ug/ml and MCF-DCIS was selected in 5ug/ml puromycin.

Clonogenic assays: 250 cells were seeded in 6- well plates overnight and the PARP1 inhibitors were added at the indicated concentrations. The plates were left in the incubator for 14 days, after incubation colonies were washed with PBS, fixed and stained with crystal violet, acetic acid and methanol mixture and counted.

Cell Proliferation assays: The effect of XRCC1 re-expression on Olaparib sensitivity in MDA-MB-157 cells was studied. 100 cells /well were seeded in 96-well plates, Left to adhere overnight. Azacytidine was added for 48 hours and then cells were treated with different doses of Olaparib for 3 days. Cell viability was measured by cell titer cell proliferation assay (MTS) (Promega, UK).

For Azacytidine studies, MDA-MB157 cells were treated with 1.5 µM Azacytidine for 48 and 72 hours. Levels of *XRCC1*mRNA were analysed by real-time PCR and XRCC1 protein expression was confirmed by western blot at indicated time points.

Cell synchronization and functional studies: Cells were seeded in 6- well plates overnight then media were changed to serum-free media for 16 hours to synchronize all the cells at G1- phase by serum starvation. The following day cells were released in complete media supplemented with 10% FBS or media containing 10uM of Olaparib for 24 hours. For studying p53 role in cell cycle regulation in response to Olaparib, cells were treated with 10µM Nutlin 3a for 48 hours. 16 hours prior to the end of the incubation, cells were synchronized in serum-free media then released and treated with 10µM Olaparib or left untreated for 24 hours. Cells were collected by trypsinization and washed with ice-cold PBS, then fixed in 70% ethanol for 30 mins. After removal of the fixative solution by centrifugation cells were labelled with phospho Histone (γH2AX) Ser139 FITC antibody. Cells were then treated with RNase (5µg/ml) and propidium iodide (10ug/ml) (Sigma Aldrich) to detect DNA in the cell cycle. For Apoptosis assay, cells were collected and analysed by Flow cytometry using AnnexinV detection kit (BD Biosciences).

Confocal microscopy: Cells were seeded on the coverslips overnight then treated with Olaparib or Talazoparib for the indicated time points. The cells were fixed with 4% paraformaldehyde for 30 mins, permeabilized with 0.1% Triton (Thermofisher) for 30 mins and blocked with 3% BSA for 1 hr. Cells were incubated with PARP1 and p- Histone

(γH2AX) Ser139 antibodies for 1 hr at room temperature. Slides were prepared in duplicates. Imaging was carried out using Leica SP2 confocal laser scanning microscope. Images were analysed in ImageJ software. For analysis minimum of 100 cells per slide were counted.

Invasion and migration assays: Cells were seeded in the Upper chamber of polycarbonate membrane inserts (8 µm pore size), (Cell Biolabs,UK) in serum-free medium and left to migrate toward 10% serum-containing medium for 24 hours. After 24 hours, medium containing non- invasive cells were aspirated from the inserts and the inner was washed with distilled water then stained with crystal violet for 10 minutes. Cells were extracted and 100 µL from each sample was transferred to a 96-well microtiter plate for measuring OD at 560nm. For migration assays, cells were seeded in 96 well plates containing a non- migratory hydrogel spot area, left to adhere overnight and then hydrogel area was digested and cells were left to migrate for 20 hours. Then the wells were washed three times, fixed and stained as per manufacturer protocol. Cell migration images were analysed by ImageJ software.

qRT-PCR analysis of epithelial-mesenchymal transition (EMT) gene expression: Real-time PCR was performed using RT^2 Profiler EMT PCR Array for 86 EMT genes. The data was analysed as per manufacturer's recommendations (https://www.qiagen.com/us/shop/genes-and-pathways/data-analysis-center-overview-page/). RPLP0 was used for normalization of the data. All experiments were performed in duplicate.

Generation of 3D spheroids: MDA-MB-231 control & XRCC1_ KO, as well as MCF-DCIS control & XRCC1_ KO, were seeded in ultra-low attachment 6-well plates using the promo cell serum-free cancer stem cells medium. After 14 days cells were fixed with formaldehyde 3.7% and stained with 2µM calcein AM and 1.5µM ethidium homodimer-1. Imaging was carried out using Leica SP2 confocal laser scanning microscope. Spheroids surface area was analysed in ImageJ software. At least 30 spheres were analysed per cell line. For MCF10-

DCIS spheres, cells were seeded as described and then treated with 10 µM Olaparib from day 0. Olaparib was refreshed every 3 days. Images of the formed 3D spheres structures were taken on day 14.

Human Invasive breast cancers: The study was performed in a consecutive series of 1650 patients with primary invasive breast carcinomas who were diagnosed between 1986 and 1999 and entered into the Nottingham Tenovus Primary Breast Carcinoma series. All patients were treated in a single institution and have been investigated in a wide range of biomarker studies (9, 10, 19, 22, 23). Supplemental Table S1 summarizes patient demographics. Supplemental treatment data 1 summarizes various adjuvant treatments received by patients in this cohort. We also evaluated an independent series of 281 ER-α negative invasive BCs diagnosed and managed at the Nottingham University Hospitals between 1999 and 2007. All patients were primarily treated with surgery, followed by radiotherapy and anthracycline chemotherapy. The characteristics of this cohort are summarised in supplementary Table S2.

The Reporting Recommendations for Tumor Marker Prognostic Studies (REMARK) criteria, recommended by McShane et al (24), were followed throughout this study. This work was approved by Nottingham Research Ethics Committee.

Tumours were arrayed in tissue microarrays (TMAs) and immunohistochemically profiled for XRCC1 (9), PARP1 (10) and other biological antibodies (Supplementary-Table S3) as previously described (19, 22, 23). Briefly, immunohistochemical staining for XRCC1 was performed using the Bond Max automated staining machine and Leica Bond Refine Detection kit (DS9800) according to manufacturer instructions (Leica Microsystems). Pre-treatment of TMA sections was performed with citrate buffer (pH 6.0) antigen for 20 minutes. TMA sections were incubated for 15 minutes at room temperature with 1:200 anti-

4

XRCC1 mouse monoclonal antibody (Ab-1, clone 33-2-5, Thermoscientific, Fremont, CA, USA) or with 1:1000 anti-PARP1 mouse monoclonal antibody (7D3-6, BD Pharmingen, USA). The tumour cores were evaluated by three specialist pathologists blinded to the clinicopathological characteristics of patients, in two different settings. There were excellent intra and inter-observer agreements ($k > 0.8$; Cohen's κ and multi-rater κ tests, respectively). Whole field inspection of the core was scored and intensities of nuclear staining were grouped as follows: 0 = no staining, 1 = weak staining, 2 = moderate staining, 3 = strong staining. The percentage of each category was estimated (0-100%). H-score (range 0-300) was calculated by multiplying the intensity of staining and percentage staining as previously described (19, 22, 23). Low/negative XRCC1 (XRCC1-) expression was defined by mean of H-score of ≤100. Low/negative PARP1 (PARP1-) expression was defined by mean of H-score of ≤10 Not all cores within the TMA were suitable for IHC analysis due to missing cores or absence of tumour cells. Data analysis was performed using SPSS (SPSS, version 17 Chicago, IL). Where appropriate, Pearson's Chi-square, Fisher's exact, Student's t and ANOVA one way tests were used. Cumulative survival probabilities were estimated using the Kaplan–Meier method, and differences between survival rates were tested for significance using the log-rank test. Multivariate analysis for survival was performed using the Cox proportional hazard model. The proportional hazards assumption was tested using standard log-log plots. Hazard ratios (HR) and 95% confidence intervals (95% CI) were estimated for each variable. All tests were two-sided with a 95% CI and a p-value < 0.05 considered significant. For multiple comparisons, P values were adjusted according to the Benjamini-Hochberg method (25).

Human ductal carcinoma in situ (DCIS): A total of 776 patients with pure DCIS diagnosed between 1987 and 2012 were identified from the National Health System (NHS) database of the Nottingham University Hospitals. A cohort of 239 DCIS that co-exist with invasive breast

cancer (IBC) as well as 50 normal breast tissues were also identified. Patients demographics including tumor grade, tumor size, age, menopausal status, screening or symptomatic presentation DCIS, histological type, presence of comedo necrosis, Paget's disease, associated lobular carcinoma in situ (LCIS) as well as local recurrence and recurrence-free interval (defined as time in months from diagnosis to the development of local recurrence) were collected. All patients received surgery. TMAs were constructed as described previously and immunostained for XRCC1. Not all cores within the TMA were suitable for IHC analysis due to missing cores or absence of tumour cells. Nuclear expression of XRCC1 within tumour cells was scored using semi-quantitatively Histo-score (H score). Staining intensity and percentage of stained nucleus and cytoplasm were considered. H score ranged from 0-300, H score obtained by multiplying staining intensity by its proportion. Low/negative XRCC1 (XRCC1-) expression was defined by median H-score of ≤120. Correlation between XRCC1 expression and different clinicopathological parameters was performed using Chi-square and Mann Whitney tests. Survival analysis versus RFI was performed used Kaplan Meier curves and compared by log-rank test. All tests were 2-tailed p-value of <0.05 was considered as significant, statistical analysis was carried out by IBM-SPSS statistical software version 21.0 (SPSS, Chicago, IL, USA). This study was approved by the North West - Greater Manchester Central Research Ethics Committee (15/NW/0685).